Tribology International 211 (2025) 110903

Contents lists available at ScienceDirect

Tribology International

journal homepage: www.elsevier.com/locate/triboint

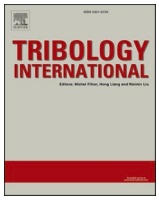

Machine learning approach to the assessment and prediction of solid particle erosion of metals

S. Brown [a], F. Khomh [b], M. Cavarroc-Weimer [c], M. Mendez [d], L. Martinu [a], J.E. Klemberg-Sapieha [a,*]

[a] Department of Engineering Physics, Polytechnique Montréal, Montréal, Quebec H3T 1J4, Canada
[b] Department of Software Engineering, Polytechnique Montréal, Montréal, Quebec H3T 1J4, Canada
[c] SAFRAN Tech, Rue des jeunes bois, Châteaufort, CS 80112, Magny-les-Hameaux 78772, France
[d] MDS Coating Technologies, 7810 Henri Bourassa Blvd W, Saint-Laurent, Quebec H4S 1P4, Canada

ARTICLE INFO

Dataset link: Dataset for Solid Particle Erosion of Metals, Machine Learning for SPE - Database and Code

Keywords:
Solid particle erosion
Machine learning
Metals
Wear

ABSTRACT

Solid particle erosion (SPE) is a tribological phenomenon in which a surface is impacted by a stream of particles, causing gradual removal of material. This poses significant challenges in aerospace, particularly when operating in harsh environments. Despite decades of data gathering and empirical model development, accurately predicting SPE remains challenging due to the complexity of the phenomenon and the variability in testing conditions. In this study, we compiled a database of over 1000 erosion tests on metals from existing studies and internal experiments, noting material properties, test conditions, and literature metadata. Machine learning (ML) models, including Random Forest, Neural Networks, Support Vector Regression, and XGBoost were employed to predict erosion rates. XGBoost was most performant, achieving a mean absolute error of 15–16 % on test data. Model performance was further validated by predicting results published in the ASTM G76 standard; predictions were within the interlaboratory standard deviation for tests at 70 m/s. Feature importance and partial dependence plots were used to evaluate the influence of different variables on erosion predictions. While particle velocity, particle size, and impact angle show the expected influence, features such as target density and Poisson's ratio showed exaggerated effects due to their role in classifying outlier materials. These results show the promise of ML for SPE prediction across a range of conditions and suggest that the broader erosion literature is valuable for quantitative predictions, while also acknowledging limitations in the ML approach, particularly where data sparsity and feature correlations hinder the accurate assessment of feature influence.

1. Introduction

Solid particle erosion (SPE) is a phenomenon in which a surface is impacted by a stream of erodent particles causing gradual removal of material and has been cited as a major issue in aerospace, wind turbines, and power generation gas or steam turbines [1,2]. It is particularly damaging to helicopter rotors and aircraft engines, where it causes wear to metallic compressor and turbine blades [2,3]; this wear changes the blade geometry and can result in significant changes in aerodynamic characteristics. Upon continued exposure, there is the additional risk of developing fatigue cracks from erosion pits. Overall, erosion results in lower engine performance, decreased efficiency, increased fuel consumption and, in severe cases, to the degradation of engine integrity [4]. This also affects operating expenses, with the cost of performance restoration for turbofan engines ranging in the millions of dollars [5].

Though SPE has been studied to some degree for over 100 years [6], there remains an imperfect understanding of how different conditions and material properties affect erosion [7]. Much work has been done on both the experimental and theoretical aspects of erosion, and many fundamental ideas and guiding principles have been established. It is well-known that the erosion of ductile materials such as metals or polymers is governed by plastic deformation and is maximized at lower angles of particle impact, whereas brittle materials like glasses or ceramics erode through the formation and intersection of cracks, with the highest erosion rates occurring at 90° impact angles where the kinetic energy normal to the surface is maximized [8]. The hardness of target materials is important, especially compared to that of the impacting particles [9], and particle size and shape will influence how much

* Corresponding author.
E-mail address: jolanta-ewa.sapieha@polymtl.ca (J.E. Klemberg-Sapieha).

https://doi.org/10.1016/j.triboint.2025.110903
Received 28 March 2025; Received in revised form 4 June 2025; Accepted 14 June 2025
Available online 16 June 2025

material is removed [10,11].

Despite the knowledge which has been gained, the complexity of SPE means that general solutions to the problem of predicting erosion remain elusive. This fact is perhaps best highlighted by a 1995 review from Meng and Ludema [12], which surveyed erosion models present in the literature and selected only those from well-cited authors with several erosion publications, whose arguments were logically consistent and whose models had been cited in a positive light in later credible papers. Still, they were able to identify 30 different erosion equations and 33 unique variables. A similar exercise carried out in 2020 increased this variable count to 46 [7]; some of these are highlighted in Fig. 1. Beyond the established guidelines, it is difficult to quantify or even qualify the importance of many material properties and erosion conditions in a general manner.

Part of the difficulty in assessing and predicting erosion comes from the fact that reported erosion rates are not intrinsic material properties, but rather the results of experiments. In practice, researchers working on SPE will perform tests under conditions representative of the real-world environments that their materials will be exposed to, and many erosion systems are custom-built or modified to achieve this goal. Though an ASTM standard, G76, exists for the gas jet erosion systems [14] and is often used as a guideline for system construction, it calls only for a low-velocity test at a single impact angle, and researchers will almost always push their testing beyond this minimum exploration. This is advantageous in terms of performing some industrially-relevant tests, but the inconsistencies in testing methodology make it "very difficult or even impossible" to directly compare the results of different studies [9].

Machine learning (ML) is well-suited for addressing this problem, solving for the influence of parameters despite variability in specific values, provided that sufficient data is available. While more significant work has been done in the oil and gas industry on using ML for slurry erosion and in pipelines [15,16], there has been a relative lack of work published on the more general case of SPE as it applies to the aerospace industry. Some studies, particularly on composite materials, have been published, but these have often been small in scale, using datasets containing less than 100 total tests, performed on a single erosion system, and accounting for very few (~5) features [17–20]. Regarding literature-based erosion studies, the most extensive work to date has been published by Liu *et al.* [21], who explored the performance of various ML models when predicting erosion of thermal barrier coatings, using a 245-instance dataset and 5 features.

The present study consists of 3 parts:

1. The creation of a database containing 1000 solid particle erosion test results for metals.
2. An evaluation of machine learning performance in predicting solid particle erosion.
3. Investigation into the impact of material properties and test conditions on model predictions.

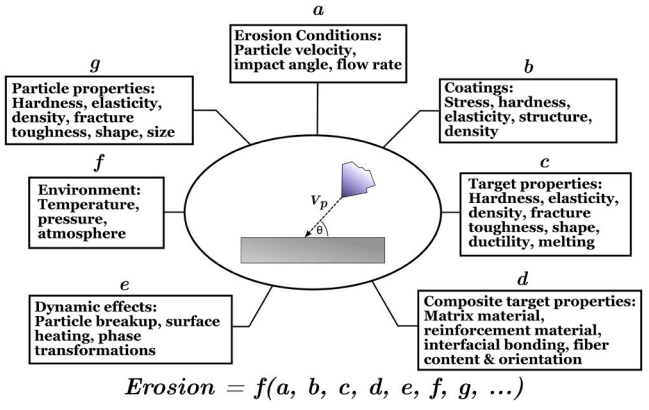

Fig. 1. Some of the factors affecting solid particle erosion. Adapted from [13].

In the first part, SPE data is compiled for use as training and test data. This data comes from the SPE literature as well as from internal tests, and tests performed by our industrial partners. A wide feature set is included, comprising a range of mechanical properties for particle and target materials, as well as system properties and literature metadata. In the second part, several ML algorithms are tested to determine the most performant for our data. The effects of increasing or decreasing the information available to the most performant model are explored, for example by treating all alloys of a given material as being equivalent. Model performance is benchmarked based on the performance on unseen test data, as well as the ability to predict interlaboratory test data included in the ASTM G76 standard. In the third part, the influence of several features on model predictions is explored using explainable ML techniques, including feature importance and partial dependence plots, and the limitations of these in terms of assessing real-world influence of different features is discussed. Our goal is to determine whether the broader literature on the solid particle erosion of metals can serve as a reliable predictor of materials performance under erosion, or if the results and test conditions are too varied, in which case the literature should be used only for qualitative comparisons.

2. Experimental

2.1. Database construction

Data on solid particle erosion rates was taken from 31 articles which cover the SPE of metallic materials [10,11,22–50], as well as from tests performed at Polytechnique Montreal and MDS Coating Technologies. While automated data scraping is useful for collecting single, well-defined properties for a given material [51,52], the large number of contributory features and the variation of their presentation from one article to another meant that data had to be gathered by hand. Data was taken directly from the text when available and extracted from graphs using the open source software WebPlotDigitizer v4 [53]. When material properties were not described in an article, they were taken from the ASM handbooks [54–71]; properties measured in the annealed state were preferred as these tend to correlate better to erosion rates [8,72]. Tertiary sources were used as required to fill out the remaining information and are listed individually in the database.

Data was assigned a "quality score" from 0 to 5. This was used as an initial indicator of how predictive a paper might be, and not as a measure of paper quality. A reason for a zero quality score may be that a paper doesn't include erosion rates and assesses erosion by other means. Reasons for a low (non-zero) quality score may include testing anomalies or important data not being reported (e.g. particle velocity, impact angle). All data points received a quality score of 5 unless there was a specific reason for this value to be lowered.

2.2. Machine learning and data organization

Several machine learning models were tested on the collected dataset including K-Nearest Neighbours, Multiple Linear Regression, Decision Trees, Random Forest, Neural Networks, Support Vector Regression, and XGBoost. For XGBoost, version 1.7.6 was used, while all other models used the implementations included in scikit-learn 1.0.2. For the Neural Networks, a multilayer perceptron architecture was used (MLPRegressor) with three hidden layers arranged in a pyramidal structure, and models were optimized by varying the hidden layer sizes, initial learning rate, and maximum number of iterations. The sci-kit learn StandardScaler was used for data scaling when comparing different model types and for variance inflation factor calculations. Data was divided into a randomized 80/20 train/test split, selected so that the mean erosion rate in the test and training data had a difference of less than

5 %. One-hot encoding was used for categorical variables. For room-temperature and high-temperature data subsets, the same randomized split was used as the full dataset (i.e., the train/test split is first applied, then each split is divided into high-temperature and room-temperature subsets). Hyperparameters were optimized for each model using GridSearchCV with 5-fold cross validation.

2.3. Erosion tests

Solid particle erosion tests were performed in a homemade system designed to comply with the ASTM G76 solid particle erosion standard [14]. The particle-gas flow originates from an Airbrasive Model H micro abrasive jet machine (S.S White). The abrasive jet machine is placed on a Sartorius LE34001S balance with a capacity of 30 kg and resolution of 0.1 g, and changes in the total mass are used to determine the mass of particles which have been sent through the system. The nozzle is made of tungsten carbide with a length of 36 mm and an inner diameter of 1.14 mm; nozzle positioning was performed via a Mecademic Meca500 robot arm. Particle velocity was calibrated to system backing pressure using the double disk method [73]. The employed particles were 50 μm angular Al_2O_3, at velocities of 30–120 ms^{-1}, and impact angles of 20–90°. A working distance of 20 ± 1 mm was used, and particle feed rate was maintained at 1.00 ± 0.25 g/min for all tests. Samples were ultrasonicated in isopropanol before and after testing, and mass difference was measured using a Sartorius LE225D analytical balance with a resolution of 0.01 mg.

3. Results

3.1. Database

The collected database comprises a total of 1010 erosion tests on metals. There are 53 distinct target materials, which includes alloys and specific heat treatments mentioned in different publications. These 53 materials can be classified into 6 “base” materials of Ti, Al, Ni, Fe, Pb, and Cu. There were 11 distinct erodent particle types identified, with the main erodents being SiO_2, Al_2O_3, and SiC. Three different types of erosion tests were also observed: gas blast, whirling arm, and wind tunnel. Of the 1010 total erosion tests, 922 had a quality score of 4 or greater and were selected for use in model training. This metric ensured that particle velocity values and a minimum amount of target and particle material properties were always available, while also allowing the inclusion of some non-standard tests, including tests with extremely large envelopes of particle sizes (1–1000 μm) [40], situations such scanning the erosion nozzle across a sample surface [34], or using large systems with particle feed rates in the hundreds of grams per minute [42].

The selection of potentially relevant material properties and erosion conditions were based on Meng and Ludema’s review covering wear equations [12], as well as the recent expansion of this published by Alqallaf *et al.* [7]. In addition to these, erosion system features encountered in the literature (e.g. nozzle dimensions, working distance, particle feed rate) were included. Table 1 shows the full list of collected database features, divided into target properties, particle properties, test conditions, and article properties. In this last case, we included the publication year and whether claims of compliance with ASTM G76 were made. These features aim to capture the context in which the tests were performed, which may influence erosion results.

The erosion values to be predicted are mass erosion rates with units mg/g, which relate the mass loss of a target material during erosion to the mass of particles to which it has been exposed. Erosion rate can also be expressed as volume loss (units mm^3/g), however this is much less common in the literature. In instances where only volume results were reported, these were converted to mass loss using the target material density.

Some data required treatment to render it consistent, for example particle sizes were modified to use single numeric values. When a size range was included, or when mesh values were used for size, the median particle size was used as the “particle size” value. Similarly, if temperature was not explicitly reported, a standard room temperature value of 21°C was used. Hardness values were primarily encountered as Vickers hardness or Rockwell hardness. Reported values were first converted to Vickers hardness following the ASTM E140–12B standard [74], and Vickers hardness values were then converted to GPa by multiplying by 0.009807, for easier comparison with internal instrumented indentation measurements. Hardness values in GPa were then used for model training and testing. Features indicating the original hardness testing technique were included in the dataset, to test whether these would affect our results. Additional information about the range of values and missing data are present in the supplementary data.

Table 1
Features included in database for SPE of metals, by property type.

Target Properties	*Particle Properties*	*Test Conditions*	*Article properties*
Material	Material	Particle Velocity	Publication year
Sample preparation	Shape	System pressure	ASTM G76 compliance
Material treatment	Size	Air velocity	
Hardness (and measurement type)	Size range	Kinetic-energy averaged velocity	
Elastic Modulus	Hardness	Incident angle	
Density	Elastic Modulus	Total erodent mass	
Poisson ratio	Density	Particle feed rate	
Ductile/brittle	Poisson ratio	Dust concentration	
Thermal conductivity	Melting temperature	Erodent flux	
Yield strength	Fracture toughness	Working distance	
Tensile strength		Nozzle diameter	
Fracture Toughness		Nozzle length	
Melting temperature		Carrier gas	
		Temperature	
		Test Pressure	
		Erosion system type	

3.2. Machine learning for SPE of metals

3.2.1. Comparison of methodologies

Machine learning tests began with a comparison of several models using a simplified version of the dataset, created by removing all features with any amount of data missing, except for impact angle. Impact angle was retained because of its significant influence on erosion, and the few cases where it was missing were handled by dropping individual tests, reducing the total to 910 datapoints. As an additional simplification, only the names of target and erodent materials were included rather than their full sets of material properties, operating under the idea that the names could be considered as an encoding of a given material’s mechanical properties. The final list of features for the simplified dataset was: Target, Erodent, Particle velocity (m/s), Particle size (μm), Incident angle (°), Temperature (°C), Test type, ASTM G76 mentioned, and Publication year. The quantitative features in the simplified database were tested for multicollinearity using variance inflation factors (VIF), as correlated features can impact the performance of linear models. A VIF value of 1 indicates no linear correlation between a feature and any other, values from 1 to 5 suggest moderate correlation, values from 5 to 10 indicate a high enough correlation with others to potentially cause issues, and values greater than 10 signify very high linear correlation that is likely to lead to problems [75,76]. In practice, any real-world variable is expected to give a value greater than 1. VIF values for all numerical features were very small, ranging from 1.07–1.25, indicating that none of our numerical variables show sufficient multicollinearity to warrant their removal from the dataset.

Seven types of model were tested: Multiple Linear Regression, Decision Trees, K-Nearest Neighbours, Random Forests, Neural Networks, Support Vector Regression, and XGBoost. In Multiple Linear Regression, a coefficient is fit to each feature, and the predicted erosion rate is the sum of the weighted features plus an intercept. There are no hyperparameters which are tuned for this model. For a Decision Tree model, a tree is built based on the most efficient splitting of the dataset based on feature values. Splitting stops either when the data cannot be split any further, or an imposed maximum tree depth is reached. All instances which finish in the same leaf get the same prediction. Optimized hyperparameters include the maximum tree depth and the minimum number of samples required to split a node further.

In K-nearest Neighbours (KNN), each feature can be thought of as a spatial dimension. To make a prediction for a new data point, its distance to every point in the dataset is calculated in this multidimensional space. The predicted erosion rate is taken as the average of the K training points with the smallest distances to the new data point, while the integer K value is optimized as a hyperparameter. A Random Forest (RF) model creates multiple decision trees, each with access to a random subset of the data and using a random subset of features at each split. The predictions of all trees are averaged to give the final predicted value. While each individual RF tree is less accurate than a single tree trained using the full data and feature set, RF models typically generalize better to unseen data. The hyperparameters tuned were the number of trees and the maximum tree depth.

Neural Networks (NNs) are models composed of interconnected layers of nodes, or neurons. The first layer consists of the input features, whose values are propagated through hidden layers which ultimately produce the predicted erosion rate. A structure with 3 hidden layers was selected to improve performance on non-linear relationships. Within each neuron, inputs from the previous layer are weighted, summed, and transformed by an activation function, allowing the network to learn complex patterns. The network's weights are adjusted during model training to minimize the error between its predictions and the actual values. Optimized hyperparameters included the hidden layer sizes, initial learning rate, and the maximum number of training iterations. In Support Vector Regression (SVR), an epsilon value is used to define the width of a "tube" around the regression trendline. Error values within this tube are considered to be zero, and error is calculated as the distance to the tube (e.g. distance to epsilon line) rather than the regression line. The objective of the model is the minimization of errors for points outside of the tube while also controlling model complexity. Different kernels can be employed to model non-linear relationships, and SVR is efficient because it can explore high-dimensional relationships without the computational expense of transforming the data to higher dimensions via the 'kernel trick'. Tuned hyperparameters included epsilon values, the employed kernel (linear, polynomial, radial basis function), kernel coefficient, and a regularization parameter C.

Finally, XGBoost is a highly optimized version of a gradient boosted decision trees algorithm. Here, an initial decision tree is made, with a limited tree depth preventing it from making very accurate predictions. A second tree is then added to the first; rather than predicting the erosion rate, this tree attempts to predict the error made by the initial tree, so that this can be corrected. The new tree is given a weight based on its ability to reduce this error. The process is repeated, with each new tree reducing the error of the previous ensemble. Additionally, XGBoost automatically handles missing feature values, uses parallel processing for tree construction, and employs regularization to prevent overfitting. The learning rate, which limits the influence of each tree, and total number of trees were optimized as hyperparameters. The list of optimized hyperparameters for all models is included in the supplementary data.

Results from each of the models are shown in Table 2. Model performance is based on the Mean Absolute Error (MAE) of predictions; for easier comparison this has been converted to a percentage value based on the mean erosion rate of the training and test data. The training error represents how well a model can predict values that it has already seen and learned from, and the test error represents how well a model can predict values for tests it has not seen. The training error tells us how capable the model is of learning from the provided data, but for practical purposes it is the test data that is used to assess model performance. Multiple Linear Regression shows large and similar errors on both the training and test data, indicating that the model is not capable of making meaningful predictions, even on data it has already seen. Multiple Linear Regression is often used in DOE-type studies to give an indication of parameter influence and has been shown in several cases to offer acceptable predictions for a small number of very similar tests [36–38], however, the non-linear relationship of erosion rate with several relevant testing parameters means that the model cannot generalize well to the larger and more complex data which has been collected. The next models are Decision Trees and K-Nearest Neighbours, which show a marked performance over MLR. Here we no longer rely on strictly linear relationships, but the training error is still relatively large, indicating that the models are not fully capturing the relationship between the input features and erosion rate even for the training data. For Random Forest, Neural Networks, and Support Vector Regression, the test error decreases to ~20 % and below, closer to the range of repeatability that we might expect to see in erosion tests performed by different laboratories [14,22]. SVR gives an improved test error with a comparatively high training error, showing good performance but indicating that we're near the limits of how well this model may perform. Finally, the XGBoost model was shown to be most performant overall, offering the same 15.8 % test error as SVR but with a decreased training error. While a large gap between training and test error can indicate overfitting, the combination of XGBoost's built-in regularization with the fact that we have a relatively small dataset indicates that the model likely has more performance to offer if more data were available. It should be noted that the values reported here represent the average absolute error divided by the average erosion rate. Some individual errors may be significantly larger than this, particularly for small erosion rates, which can exhibit comparatively larger relative errors.

Table 2
Performance of ML models on simplified database.

Model	***MAE, as % of ER Mean***	
	% Error Train	% Error Test
Multiple Linear Regression	60.8	**64.3**
Decision Trees	16.4	**30.2**
K-Nearest Neighbours	15.1	**30.1**
Random Forest	8.6	**21.9**
Neural Networks	11.6	**19.1**
Support Vector Regression	11.6	**15.8**
XGBoost	3.4	**15.8**

The size of the dataset also has a large effect on model performance. To test this, we trained our optimized models on subsets of the training data from 5 % to 100 %, and then tested their predictions on the subset training and full test datasets. A comparison of these results for XGBoost and SVR are shown in Fig. 2, where MAE (in mg/g) is plotted as a function of training dataset size. As is typical, the models trained on small amounts of data overfit the training data, giving excellent predictions for erosion scenarios they have seen but completely failing to generalize to different conditions. As the amount of training data increases and the model has seen a larger and more representative set of data, it is less able to fit this perfectly but generalizes better to the unseen test data. Consequently, the performance gap between predictions on the training and testing datasets decreases as more data becomes available. Ultimately, the training results serve as an upper bound on the model's performance when applied to unseen data. It can thus be seen in Fig. 2 that the SVR model is close to its maximum level of performance on this dataset, while the XGBoost model would likely benefit from more data if it were available. Curves for all tested models are available in the

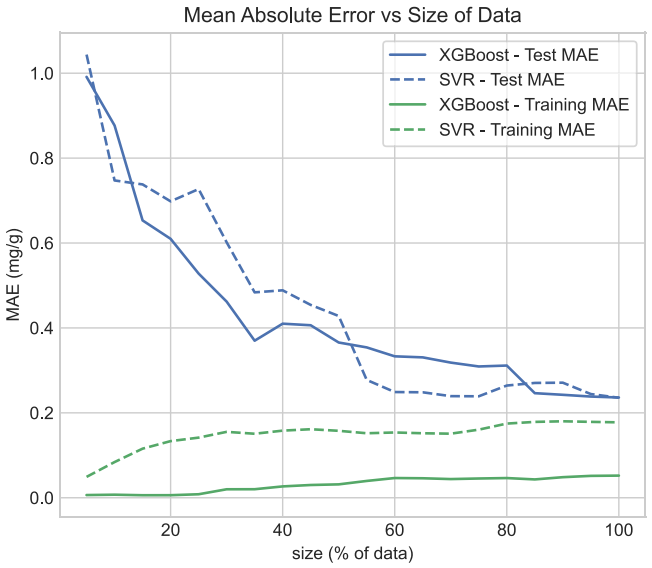

Fig. 2. The effect of adding more training data on the training and test MAE for XGBoost and support vector regression models.

Supplementary Data.

3.2.2. Testing on complete SPE database

Given the performance of XGBoost on our simplified dataset, this model type was selected to continue testing on the complete SPE database. We began by experimenting with the effect of including or removing different pieces of information in the database, creating 3 different scenarios:

1. Using target and erodent names only
2. Using the base target material and erodent names only
3. Using materials properties only, with no material names

The first case is similar to what was shown in the previous section, but includes features which are present in at least 50 % of test cases, adding particle shape, nozzle diameter, and carrier gas to the data. Rather than removing erosion results with missing feature values, XGBoost's built-in handling for missing data was used, which gives a set of 922 datapoints after removing data with a low quality score. In the second scenario, targets are renamed to consider only the base target materials, so that all titanium alloys become "Ti", all steels become just "Steel", all aluminum alloys become "Al", etc. It has been shown that alloys in a given family tend to have similar erosion rates [8,77], so here we test whether the additional data gained for each "class" of material would offset the additional noise added by considering these materials to all be the same when making predictions. The final case is the most interesting for application, where the names of all materials are removed, and the material properties are added. This would allow researchers to make predictions about theoretical metals without necessarily assigning them to an existing class of materials. Of course, these theoretical metals would have to erode in a similar fashion to existing metals for predictions to be accurate.

In each of the three cases above, we also explored several conditions to better understand how they affect predictions, re-optimizing the model for the specific task at hand in each case. These, along with the relevant train and test errors, are shown in Table 3. Beginning with the case of the main model, it is seen that models perform similarly to the simpler model from the previous section, with fluctuations but no major changes to the results between the three scenarios. We next explored whether there was any effect of treating the labels for SiO_2, ARD (Arizona Road Dust), and Quartz as equivalent, given that Quartz is a form of SiO_2 and ARD is primarily composed of SiO_2, although they are not necessarily identical in composition or behavior. Again, no major change is seen for the first two scenarios; this set of conditions is not applicable to the third scenario, as it is not using erodent names as a feature. The next two scenarios cover splitting the data into room temperature (RT, $\leq$ 31 °C) and high temperature (HT, $>$ 31 °C) subsets. Given that we have much more room temperature (749 datapoints) than high temperature (173 datapoints) data, it is not surprising to see that model performance is better for the room temperature tests across the board. Room temperature results also consistently outperform the "Main model" results, which makes sense given that this combines both the RT and more error-prone HT data. This is particularly true for the second scenario, which suggests that the increase in available data due to the grouping of similar materials is having a greater effect than any additional noise in the data cause by considering similar materials to be identical. It may be noted that the RT and HT test results are both slightly better for the second scenario compared to the first, while the "Main Model" performance of the first scenario is slightly better than the second. This seemingly contradictory quirk comes from the fact that we are training a new model in each of these cases, rather than using the "Main Model" to only predict RT or HT results. For HT results the material-properties-only model showed a marked improvement over the two others. It is tempting to believe that this is due to the inclusion of temperature-specific properties such as melting temperature or thermal conductivity, however, removing each or even both of these properties during training did not have a large effect on predictions. More likely, this model is better able to classify similarly-behaving materials without requiring that they share the same name.

Table 3
Train and Test mean absolute error with changing data availability.

Test set	*Target/Erodent Names only*		*Base Target Material, Erodent names only*		*Material Properties only*	
	% Error Train	% Error Test	% Error Train	% Error Test	% Error Train	% Error Test
Main model	3.4	**15.4**	3.7	**15.5**	3.1	**15.9**
SiO_2 = = ARD = = Quartz	3.3	**15.5**	3.3	**15.5**	N/A	N/A
RT Only	3.4	**14.1**	2.0	**13.3**	2.5	**15.0**
HT only	11.3	**28.7**	11.5	**27.0**	13.1	**25.4**

Each of the main models can be further examined by plotting the actual erosion rates in the test set vs the model's predictions and the associated residuals, shown in Fig. 3. For a perfect model, all of the data points would appear on the black y = x line for the actual vs. predicted graph, and the y = 0 line of the residual plot. The dotted lines represent a deviation equal to the errors reported in Table 3 to give a more intuitive sense of how well the data falls within these bounds. In all cases we can see that most of the error is coming from smaller erosion rates whose error values are not large in absolute terms, but which are large relative to their values. There is also a single large outlier which is being underpredicted in every case. This value (41.95 mg/g) represents by the far the largest erosion rate in the database, for an Al alloy being eroded in a whirling arm system at a velocity of 542 m/s. Such large velocities are extremely difficult to achieve in the more common jet blast type of erosion system, leading to data scarcity in this region. The next highest erosion rates—29.66 mg/g and 32.08 mg/g—come from similar tests on Ni and Ti alloys and were included in the training data. This consistent underprediction likely reflects a limitation of trees-based models such as XGBoost, which can struggle to extrapolate to values outside the ranges found in the training data.

Overall, we see that the predictions are quite consistent for the three models, especially for scenarios 1 and 2, and that despite relatively large errors for some tests with small erosion rates, the majority of the data falls within the bounds of the average error spread: 56.2 %, 56.2 %, and 60.5 % of the data has a smaller error value than the Table 3 values for

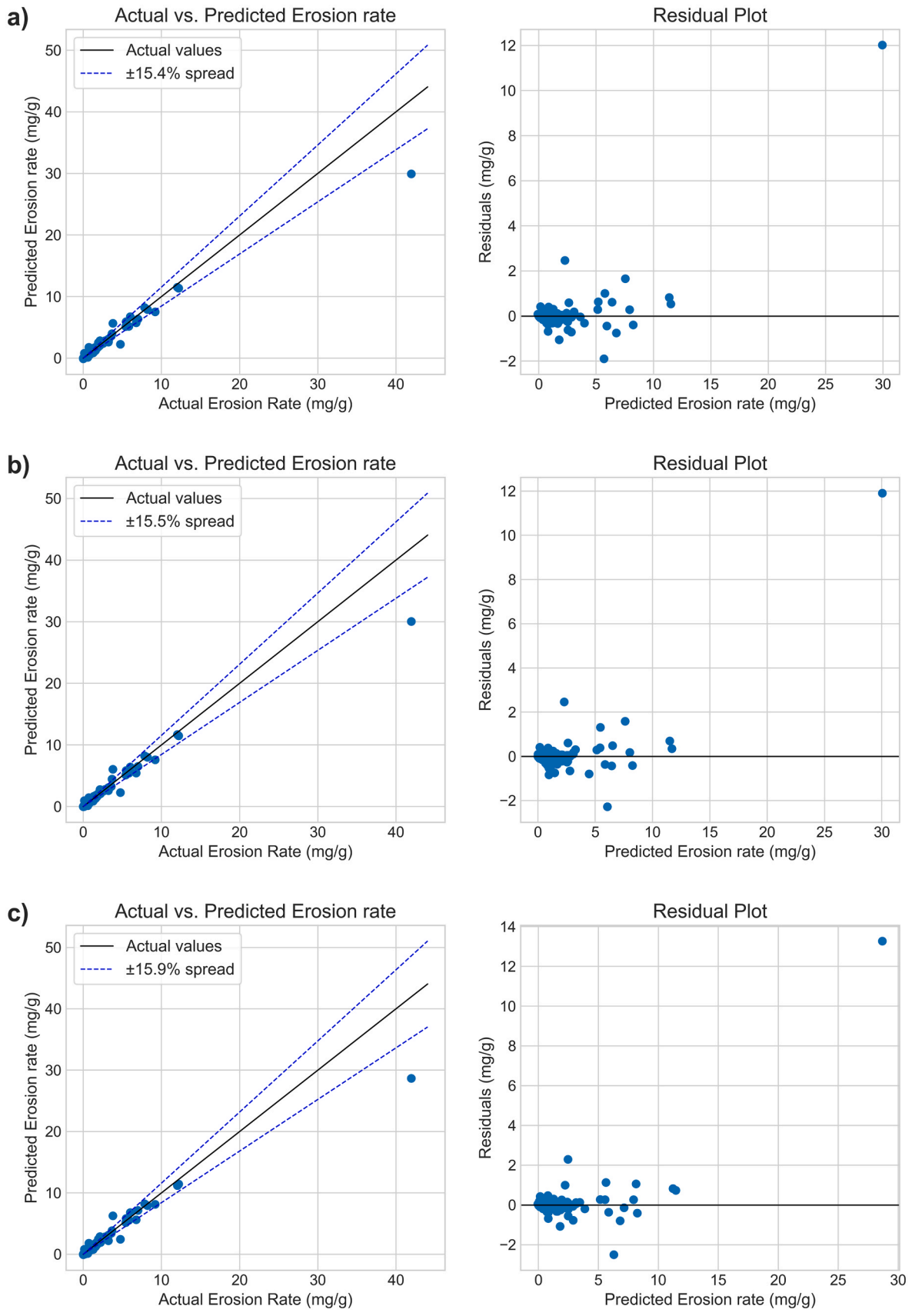

Fig. 3. Actual vs predicted values of erosion rate for test set and residuals for a) target and erodent names-only, b) target base names only, and c) material properties only test cases.

scenarios 1, 2, and 3, respectively. The fact that these values are greater than 50 % indicates that we have a slight skew towards more but smaller error values within our MAE bounds, and fewer but larger errors outside of these bounds.

3.2.3. Comparison of interlaboratory test results reported in ASTM G76 with model predictions

While the above results give a sense of overall model performance, they are not fully satisfying in terms of showing real-world quantitative predictions outside of the gathered dataset. To address this, we decided to directly compare our model's predictions to what should be the most reliable source of data possible: the interlaboratory test results provided in the ASTM G-76 standard. In these tests, 5 laboratories performed 4–10 replicates of the tests identified in Table 4; for brevity, only some conditions are listed, all others are as instructed in the standard. Predictions were made using the three model scenarios described in the previous section, trained on the full database of erosion results. Notably, the training dataset did not include any instances of either 1020 steel or stainless steel 304 being eroded by Al_2O_3, though it did contain instances of both materials being eroded by larger (175–355 μm) SiC particles.

A comparison of the predictions with the actual results are shown in Fig. 4. The error bars represent the published between-laboratory standard deviation for the tests, rather than the smaller within-laboratory standard deviation. We believe that this is the more appropriate benchmark, as our model is learning from "between-laboratory" type tests. For the 1020 Steel test at 30 m/s, the scenario 1 names-only model gives an accurate prediction, while predictions from both the scenario 2 and 3 models are much too large, 8–9 times greater than the actual result. Some explanation for this discrepancy can be found by looking further at the database itself. For the scenario 1 model, each target material is distinct, and as such it is expected to base its predictions on the other 1020 steel results in the database, without influence of other similar materials. In fact, all of these results come from a single source [44] which employs relatively low particle velocities (an average of 67 m/s) compared to the rest of the database (average of 136 m/s).

The similar performance between the scenario 2 and 3 models suggests that using the mechanical properties of the target material has an effect similar to grouping all steels together. This is expected as the properties of a given steel are generally more similar to other steels than to materials like titanium or aluminum. This improves the ability to generalize but can also introduce other biases. Looking at the subset of all steels, the 238 tests have an average particle velocity of 175 m/s, and only 1 result comes from tests performed in the 20–40 m/s range: a test on 1020 steel performed at 37 m/s. The scenario 1 model thus has a highly relevant piece of data to learn from with few other conflicting sources of information; it is highly biased, but in a way that is convenient for this specific prediction. On the other hand, low-velocity erosion is under-represented for the aggregated steel results in the scenario 2 model. The scenario 3 model fares slightly better, with its more nuanced description of target materials, but the relatively small number of low-velocity tests in the database (21 total tests in the 20–40 m/s range) is likely affecting its performance as well.

Moving to the higher-velocity 70 m/s tests, the opposite effect is observed. Here both the scenario 2 and 3 models give very accurate predictions, within the between-lab standard deviations, while the scenario 1 model is either too low or too high. The predictions of the scenario 2 model are of course the same for each material since it treats both as simply "steel", however, we end up with a slight difference when converting the predictions made in units of mg/g to the mm^3/g values used in ASTM G76, due to the difference in density of the 2 steels. The scenario 3 model is a little more nuanced, and correctly predicts a higher average erosion rate for stainless steel 304, though this difference is still smaller than the between-lab SD. Unexpectedly, the scenario 1 model underestimates the erosion rate for 1020 steel at 70 m/s, despite the presence of similar data in the database. This discrepancy may be due to differences in the erodent type and particle size affecting the model's prediction. Finally, the overestimation of stainless steel 304 by the scenario 1 model likely relates to the high velocities of the limited relevant data in the database, where most tests were conducted at velocities above 150 m/s, with only one test below 100 m/s.

Table 4
Conditions employed in ASTM Interlaboratory tests.

Eroded Material	*Erodent*	*Shape*	*Size (μm)*	*Velocity (m/s)*	*Incident angle (°)*
Steel – SAE 1020	Al2O3	Angular	50	30	90
Steel – SAE 1020	Al2O3	Angular	50	70	90
Stainless Steel 304	Al2O3	Angular	50	70	90

3.3. Assessment of parameter influence

Next, we sought to gain a deeper understanding of how the model makes decisions. Although XGBoost is a trees-based method, it is also an ensemble method which combines predictions from a large number of trees, each of which is a weak learner on its own. This means that interpretability is sacrificed, and explainable ML tools are required. These tools allow us to probe a model, however, it must be understood that they provide only information on how a model makes predictions, and that this is not guaranteed to be physically meaningful. This section focuses on the material-properties-only model, as this provides the most information about the influence of different features.

Before looking at the model itself, we calculated VIF values for the full material-properties-only dataset. As XGBoost produces non-linear trees-based models, our model will not have the same susceptibility to multicollinearity in the dataset as linear regression-based models. That being said, we expect several of the material properties values to be correlated and as such would like to quantify this. As previously, particle size, particle velocity, incident angle, temperature, and publication year all show low values, ranging from 1.26–2.52; nozzle diameter is added to the system conditions and gives a similarly low value of 1.66. While multicollinearity remains low for these categories, there is an increase compared to the simplified dataset. In the earlier case, the categorical variables for the target and erodent materials were excluded from the VIF calculation. Replacing these with numerical values representing their material properties means that the erodent and target materials are now explicitly accounted for, and the higher VIF value may suggest weak but existing correlations between these features and the types of materials being used. We start to see very strong correlation for the erosion target properties, with several values in the 10–25 range, and the largest values for target yield strength (94.53) and target tensile strength (124.15) which are of course highly correlated. The situation is even more extreme for the erodents, with VIF values over 100 for density, hardness, and melting temperature, and over 4000 for Young's modulus and fracture toughness. This clearly does not prevent the model from making accurate predictions but portends some difficulty in determining the true influence of each feature.

Returning to the model itself, Fig. 5 shows a feature importance chart, which quantifies how often a feature is used to split data across all trees in the model. We see immediately that Velocity, Target hardness, Particle size, Target elastic modulus, and Erodent hardness are the most important features. This aligns well with ideas in the literature about the dominant features in SPE, however, we must be cautious with these results. Feature importance tends to be biased towards features with more unique values, as these will often be used in splits even if other features offer more predictive power. This is especially the case for Velocity and Particle size, where a wide range of values are represented in the database. Feature importance also does not give any sense of how

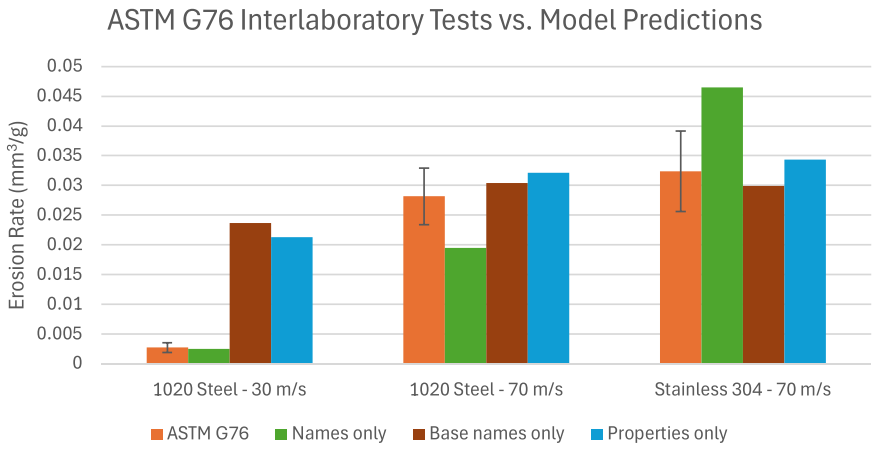

Fig. 4. Comparison of interlaboratory test results reported in ASTM G76 with model predictions. Error bars represent the between-laboratory standard deviation.

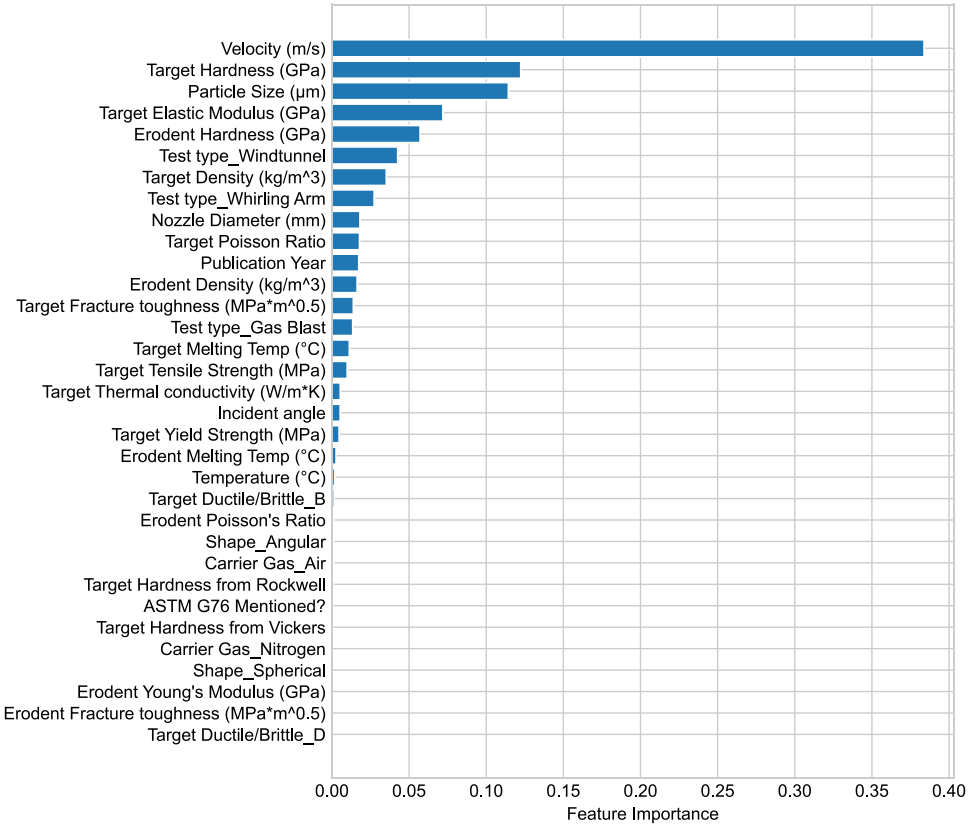

Fig. 5. Feature importance for model trained on full dataset, indicating how often a feature is used to split data.

a given feature is affecting predictions (i.e., whether it has a positive or negative impact on erosion rate).

Our understanding of the model can be further improved using partial dependence plots (PDP, Fig. 6). These plots give an idea of how the model's average prediction would vary if one feature was changed while all others remained the same. This assumes that all features are independent, which from our VIF results is of course not true for such a dataset. That being said, PDPs give us more information about our model, if not necessarily capturing the physical reality, and allow us to better quantify the influence of our most important features.

Fig. 6 contains PDPs for the most influential features, while the full set can be found in the supplementary data. The plots are ordered by feature importance, and it is immediately clear that while more important features can have a larger effect on erosion predictions, this is not always the case. We first see the exponential relationship between erosion rate and velocity, with a fitted dependence of $ER \propto V_p^{1.99}$. This value is lower than what is typically reported, where exponents for the erosion of metals are generally in the range of 2.2–2.4 [78]. This can partially be explained by the data available, and the model being employed. Because XGBoost is a trees-based model, it will make splits at discrete velocity values (i.e., one tree may make a decision based on whether $V_p < 100\ m/s$, and a subsequent tree may then make a decision based on whether $V_p > 50\ m/s$). Since our velocity values are relatively sparse in certain ranges (see histogram in Fig. 7), we end up with a step-like function for velocity dependance. In ranges where the values are particularly sparse, e.g., $V_p = 160–220\ m/s$, we first get a plateau, followed by a large jump and then a sudden smaller decrease. This tells us that our model will likely underpredict erosion rates for velocities

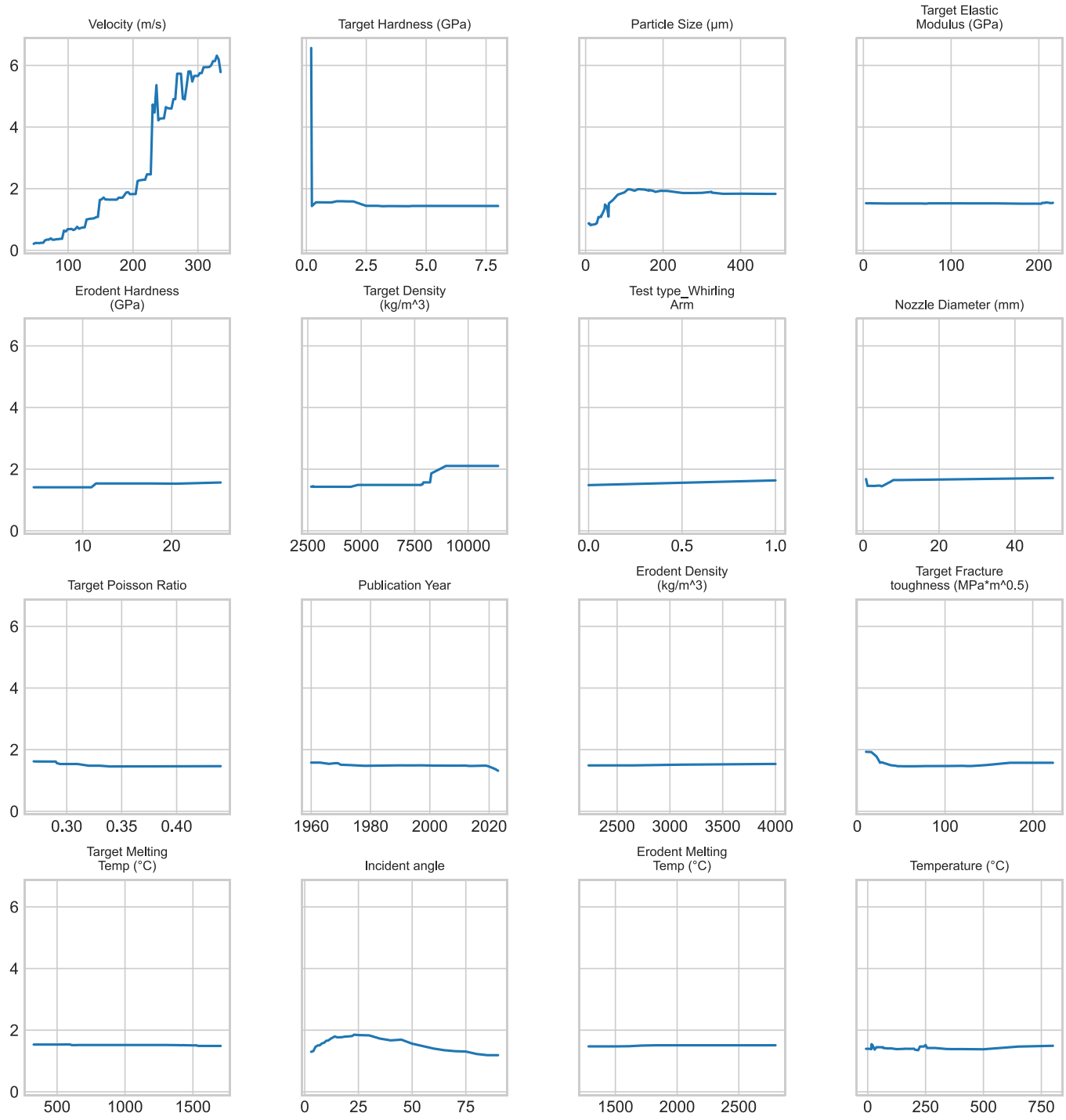

Fig. 6. Partial dependence plots for most influential features, indicating the effect of each on predicted erosion rate.

between ~160 m/s and 220 m/s, which contributes to the decreased velocity exponent.

We can next look at the dependence on Erodent and Target hardness. Erodent hardness is basically split into 2 classes centered around ~11 GPa: soft and hard. Erodents with a hardness below 11 GPa (e.g., glass, Arizona road dust) give a lower prediction. The step into "hard" erodents occurs at 11.5 GPa, which is the value used for Quartz and SiO_2, and erosion rate continues to increase slightly beyond this. The model is thus making a clear distinction between ARD and pure SiO_2-based materials. We may expect a larger effect of hardness for Al_2O_3 and SiC as compared to SiO_2; this effect appears to be split among the correlated features of erodent density and melting temperature, though it is also long-established that once particle hardness significantly exceeds target hardness, further increases will have a diminishing effect [44].

Target hardness, on the other hand, shows an enormous increase in erosion rate at very low hardness. This point in particular highlights the reason for evaluating the effect of a feature rather than just looking at its importance. Here the model is predicting very large erosion rates for very low hardness values, followed by a steep drop-off, and then a smaller drop-off as material hardness increases past 2 GPa. While the trend is logical (softer materials are eroding more), the specifics are clearly non-physical. What is happening here is that the model is using hardness as a classifier for Pb, which is a unique material in the dataset:

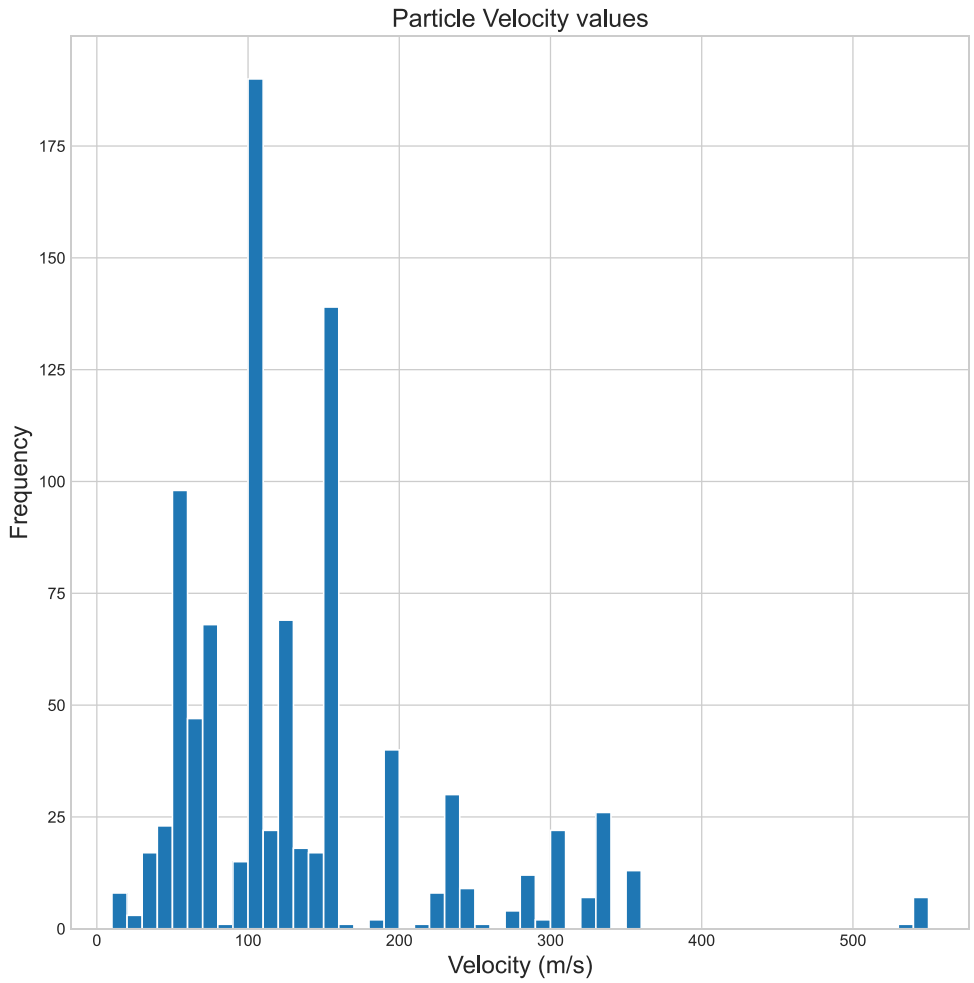

Fig. 7. Histogram of particle velocity values in the dataset. Note the multiple bins with a low number of values between 160 and 260 m/s.

it is much softer, denser, and has a higher Poisson Ratio than all other materials, and it also has a much higher erosion rate. The model is essentially using the lowest hardness value to determine that the material is Pb, and then is greatly increasing its predicted erosion rate as a consequence. Similar effects are seen for the correlated Target density and Target fracture toughness features, while Target Poisson ratio seems to be employed as a small correction factor, decreasing the Pb erosion rate slightly.

Two other features merit discussion in particular detail: Particle size and Incident angle. For Particle size, we see an increase in erosion rate as particles get bigger, up until a maximum of around 100 μm, after which the influence of this feature begins to taper off. This is extremely consistent with what is reported in the literature, though the reason for this is not well understood [10,46,78]. The PDP for Incident angle shows an increase from 0° up until a maximum at 20–30°, followed by a decrease of erosion rate as the angle increases further. This is a textbook description of how erosion rate varies with incident angle for metals, where material removal efficiency is shown to be highest at lower angles. It must be noted that the database contains multiple tests where the effects of particle size and incidence angle were being tested explicitly, so it's not shocking that the model is able to capture their general influence. It is also very helpful to the model that these were tested over a range of values, which allows the relatively smooth curves with fewer steps than were observed for Particle velocity. That being said, the consistency of these results is quite stunning when considering the variety of the current database and indicates broad agreement in the literature on the effect of these features in a way that is otherwise difficult to quantify.

Several other features show a smaller but still interesting influence on erosion rate. Predictions were slightly larger for whirling arm type erosion systems compared to gas blast systems or wind tunnels. Erosion rate also tended to increase a small amount with nozzle diameter, while decreasing with publication year. While publication year is clearly having some influence on predictions, attempts at interpretation should be cautious. The data is relatively sparse between the years 1975 and 2010, meaning the lack of noise in this section can be interpreted as a lack of data rather than consistency among all results. Nevertheless, it is clear that predicted erosion rates before 1975 tend to be larger, especially when compared to the most recent results, which may be due to a lack of standardization in testing systems and particle size distributions in the early days of SPE testing. There is no clear relationship between predicted erosion rate and test temperature, aside from a small increase beyond 500 °C. Erosion rate may increase or decrease with test temperature depending on the material being used, and has been correlated to the melting temperature of the material [27,79], so a generalized trend is not expected to emerge. At higher temperatures, oxide formation becomes more likely, and this will increase erosion rates if the oxide is non-protective [22,80,81]. Erosion rate predictions decreased slightly with increasing target melting temperature and increased slightly with increasing erodent melting temperature, though the effect of this was much smaller than the properties mentioned above. Several other features, such as carrier gas, a marker for ductile or brittle-type erosion, stated ASTM G76 compliance, target thermal conductivity, the hardness test type for the target, erodent fracture toughness, and even erodent shape did not show a meaningful effect on erosion prediction. In some cases this is due to a lack representation in the data: there were only 34

tests performed with spherical particles vs. 888 for angular particles, and the feature importance graph shows us that the Shape parameters, particularly "Shape_Spherical" are very rarely used. Similarly, there were only 16 tests which produced an erosion curve typical of a brittle material (for Quenched Carbon Tool steel and Grey Cast Iron), while the remainder were labelled with the ductile behaviour typical of most metals.

3.4. Other tests

3.4.1. Numerical encoding of categorical features and different imputation techniques

To further look at the influence of categorical features, a model was trained using numerical encoding of the particle shape, carrier gas, test type, and target ductile/brittle features rather than one hot encoding used in the original model. This technique assigns an integer to each value (e.g. for the test type, "Gas Blast" becomes 0, "Wind tunnel" becomes 1, "Whirling Arm" becomes 2), permitting easier identification of feature influence in PDP charts. Carrier gas saw a large increase in feature importance, but did not show any real change in prediction values when air or nitrogen was used. Test type retained a high feature importance; gas blast and wind tunnel tests gave similar predictions whereas a whirling arm system resulted in a 12 % increase in predicted erosion rate. Target ductility saw an increase in feature importance with brittle targets predicted to experience 10 % more erosion on average. Particle shape was the least affected, showing neither a large feature importance nor any meaningful change in predictions between angular and spherical particles.

Lastly, we evaluated various imputation techniques to handle missing data in the database and compared their performance to XGBoost's built-in handling. Specifically, we tested filling all missing values with the mean of each feature, filling with random values within each feature's range, and using the IterativeImputer class in scikit-learn. The latter employs Multivariate Imputation by Chained Equations (MICE) to estimate missing values based on all other available data [82]. XGBoost's built-in handling was the most performant in all cases, producing train/test errors of 3.1 % and 15.9 %, respectively. The mean-value imputation was not too much worse, giving a training error of 4.1 % and a test error of 16.3 %, while the random-value imputation tended to overfit the training data with a training error of 1.8 % and a test error of 18.1 %. The IterativeImputer results were very similar to the built-in handling at 2.9 % and 16.2 %. Overall, the lack of distinct improvement and the extra effort required to implement alternative imputation schemes means that the best option was to let XGBoost handle the missing data directly.

4. Conclusions

In this work, a database of test results for the solid particle erosion of metals was gathered from the literature and from internal tests, and machine learning was applied to assess erosion predictability. The database included an extensive feature set including target properties, erodent properties, test conditions, and article metadata. Several machine learning algorithms were applied to a simplified dataset that included the principal identified erosion condition parameters, with target and erodent names used to encode their physical properties. This dataset was found to be free of multicollinearity issues making it suitable for use with any type of ML algorithm. Of the tested algorithms, XGBoost was found to be most performant. Several tests were then performed with XGBoost models trained using target and erodent names only, the base target material and erodent names only, and materials properties only. Mean absolute error was in the range of 15–16 %, and all models performed better when predicting room temperature rather than high temperature erosion rates, not surprising given the database's bias towards room temperature tests. The source of error was shown to be primarily tests which had low erosion rates, and more than 50 % of the predictions were withing the reported error range in each case.

To better quantify model performance beyond percentage errors based on the mean erosion rate, predictions were made based on the interlaboratory tests published in the ASTM G76 standard. The erosion rate predicted by the model using only material properties was much too large for the 30 m/s test, but predictions were withing between-lab standard deviation for the 70 m/s tests. Feature importance and partial dependence plots were used to better understand model predictions. Particle velocity was the most influential feature, with a $ER \propto V_p^{1.99}$ dependence fit to the PDP data. The influence of particle size and incident angle used by the model was in excellent agreement with what has been shown in the literature. The effect of target hardness was overstated due to its ability to effectively classify Pb, the softest and most erosion-prone material in the database; the influence of some other features was also exaggerated in this same way. Features such as particle shape and target brittleness were found to not be very influential to model predictions, though numerical encoding helped assess the impact of some categorical features.

Overall, the model was able to make reasonable predictions about erosion rates, even for target/erodent combinations not included in its training data. This shows that despite the difficulty of direct comparison between individual erosion publications, the data contained in the broader erosion literature offers a basis for quantitative predictions, and that machine learning can be used to leverage patterns within the data to account for the variability in testing conditions, materials, and methodologies present in individual studies. In future publications it would be interesting to perform further testing with other model types, in particular physically-informed models which could prevent the overemphasis of features that act as strong classifiers for outlier materials, and to guide the individual influences of correlated features. Expanding the present database to include more tests using spherical particles and high temperatures would also improve any model's ability to generalize to the broader set of conditions encountered in real-world environments.

Statement of originality

The authors hereby declare that the present original work has not been previously published, nor is it under consideration for publication by any other journal. All authors have checked the manuscript and agreed to its submission.

CRediT authorship contribution statement

Stephen Brown: Conceptualization, Methodology, Investigation, Software, Visualization, Data curation, Formal analysis, Writing - original draft, Writing - review & editing. **Foutse Khomh:** Conceptualisation, Methodology, Writing - review & editing. **Marjorie Cavarroc-Weimer:** Writing - review & editing, Resources, Funding acquisition. **Manuel Mendez:** Writing - review & editing, Resources, Funding acquisition. **Ludvik Martinu:** Writing - review & editing, Supervision, Resources, Funding acquisition. **Jolanta E. Klemberg-Sapieha:** Writing - review & editing, Supervision, Resources, Funding acquisition

Declaration of Competing Interest

The authors declare that they have no known competing financial interests or personal relationships that could have appeared to influence the work reported in this paper.

Acknowledgements

The authors wish to thank Dr. Amin Nikanjam and Dr. Edern Menou for fruitful discussions, Mr. Francis Turcot and Mr. Francis Boutet for expert technical assistance, and Mr. Joel Restrepo-Vermette for assistance in data collection. This project has been supported by the Natural

Sciences and Engineering Research Council of Canada (NSERC), the Pôle de Recherche et d'Innovation en Matériaux Avancés du Québec (PRIMA Québec), MDS Coating Technologies and the Safran Group through NSERC grant # ALLRP 571799-21, and PRIMA Québec grant # R23-13-003.

Appendix A. Supporting information

Supplementary data associated with this article can be found in the online version at doi:10.1016/j.triboint.2025.110903.

Data availability

Links to data and code shared at the "attach file" step, and are present in the text

Dataset for Solid Particle Erosion of Metals (Zenodo)
Machine Learning for SPE - Database and Code (GitHub)

References

[1] Bousser E, Martinu L, Klemberg-Sapieha JE. In situ real-time solid particle erosion testing methodology for hard protective coatings. Surf Coat Technol 2013;237:313–9. https://doi.org/10.1016/J.SURFCOAT.2013.06.128.
[2] Wang G, Jia X, Li J, Li F, Liu Z, Gong B. Current State and Development of the Research on Solid Particle Erosion and Repair of Turbomachine Blades. In: Nee AYC, Song B, Ong S-K, editors. Re-Engineering Manuf. Sustain. Singapore: Springer Singapore; 2013. p. 633–8. https://doi.org/10.1007/978-981-4451-48-2_103/COVER.
[3] Bousser E. Solid particle erosion mechanisms of protective coatings. Aerosp Appl Polytech Montr 2013.
[4] Yang Q, Seo DYY, Zhao LRR, Zeng XTT. Erosion resistance performance of magnetron sputtering deposited TiAlN coatings. Surf Coat Technol 2004;188–189:168–73. https://doi.org/10.1016/j.surfcoat.2004.08.012.
[5] Shannon A. Aircraft Maintenance Handbook For Financiers. first ed. Aircraft Monitor; 2018. ⟨www.aircraftmonitor.com⟩ (accessed November 28, 2021).
[6] Reynolds O. XLII. On the action of a blast of sand in cutting hard material, London, Edinburgh. Dublin Philos Mag J Sci 1873;46:337–43. https://doi.org/10.1080/14786447308640953.
[7] Alqallaf J, Ali N, Teixeira JA, Addali A. Solid particle erosion behaviour and protective coatings for gas turbine compressor blades-a review. Processes 2020;8:984. https://doi.org/10.3390/pr8080984.
[8] Hutchings I, Shipway P. Wear by hard particles. Tribol. Frict. Wear Eng. Mater. 2nd ed. Elsevier Ltd; 2017. p. 165–236. https://doi.org/10.1016/b978-0-08-100910-9.00006-4.
[9] Bousser E, Martinu L, Klemberg-Sapieha JE. Solid particle erosion mechanisms of protective coatings for aerospace applications. Surf Coat Technol 2014;257:165–81. https://doi.org/10.1016/j.surfcoat.2014.08.037.
[10] Tilly GP. A two stage mechanism of ductile erosion. Wear 1973;23:87–96. https://doi.org/10.1016/0043-1648(73)90044-6.
[11] Bahadur S, Badruddin R. Erodent particle characterization and the effect of particle size and shape on erosion. Wear 1990;138:189–208. https://doi.org/10.1016/0043-1648(90)90176-B.
[12] Meng HC, Ludema KC. Wear models and predictive equations: their form and content. Wear 1995;181–183:443–57. https://doi.org/10.1016/0043-1648(95)90158-2.
[13] Kedir N, Gong C, Sanchez L, Presby MJ, Kane S, Faucett DC, et al. Erosion in gas-turbine grade ceramic matrix composites. J Eng Gas Turbines Power 2019;141. https://doi.org/10.1115/1.4040848.
[14] ASTM-G76, Test Method for Conducting Erosion Tests by Solid Particle Impingement Using Gas Jets, (2013). https://doi.org/10.1520/G0076-13.
[15] Prashar G, Vasudev H. Application of artificial neural networks in the prediction of slurry erosion performance: a comprehensive review. Int J Interact Des Manuf 2024:1–19. https://doi.org/10.1007/S12008-024-02014-7/FIGURES/16.
[16] J. Zhang, J.(Yijie,) Li, W. Pei, S. Shirazi, Physics-Informed Data Augmentation of Experimental Erosion Data Through Generative Adversarial Networks, (2024). https://doi.org/10.1115/FEDSM2024-130858.
[17] Zhang Z, Friedrich K. Artificial neural networks applied to polymer composites: A review. Compos Sci Technol 2003;63:2029–44. https://doi.org/10.1016/S0266-3538(03)00106-4.
[18] Patnaik A, Satapathy A, Mahapatra SS, Dash RR. A modeling approach for prediction of erosion behavior of glass fiber-polyester composites. J Polym Res 2008;15:147–60. https://doi.org/10.1007/s10965-007-9154-2.
[19] Rout AK, Satapathy A. Study on mechanical and tribo-performance of rice-husk filled glass-epoxy hybrid composites. Mater Des 2012;41:131–41. https://doi.org/10.1016/j.matdes.2012.05.002.
[20] Kumar Padhi P, Satapathy A. Solid particle erosion behavior of BFS-filled epoxy-SGF composites using taguchi's experimental design and ANN. Tribol Trans 2014;57:396–407. https://doi.org/10.1080/10402004.2013.877178.
[21] Liu Y, Ravichandran R, Chen K, Patnaik P. Application of machine learning to solid particle erosion of APS-TBC and EB-PVD TBC at elevated temperatures. Coatings 2021;11:845. https://doi.org/10.3390/coatings11070845.
[22] Zhou J, Bahadur S. Erosion-corrosion of Ti-6Al-4V in elevated temperature air environment. Wear 1995;186–187:332–9. https://doi.org/10.1016/0043-1648(95)07161-X.
[23] Yerramareddy S, Bahadur S. Effect of operational variables, microstructure and mechanical properties on the erosion of Ti-6Al-4V. Wear 1991;142:253–63. https://doi.org/10.1016/0043-1648(91)90168-T.
[24] Emiliani M, Brown R. The effect of microstructure on the erosion of Ti-6Al-4V by spherical particles at 90° impact angles. Wear 1984;94:323–38. https://doi.org/10.1016/0043-1648(84)90134-0.
[25] Smeltzer CE, Gulden ME, Compton WA. Mechanisms of metal removal by impacting dust particles. J Fluids Eng Trans Asme 1970;92:639–52. https://doi.org/10.1115/1.3425091.
[26] Wei R, Rincon C, Langa E, Yang Q. Microstructure and tribological performance of nanocomposite Ti–Si–C–N coatings deposited using hexamethyldisilazane precursor. J Vac Sci Technol A Vac Surf Film 2010;28:1126–32. https://doi.org/10.1116/1.3463709.
[27] Gat N, Tabakoff W. Some effects of temperature on the erosion of metals. Wear 1978;50:85–94. https://doi.org/10.1016/0043-1648(78)90247-8.
[28] Grögler T, Plewa O, Rosiwal SM, Singer RF. CVD diamond films as protective coatings on titanium alloys. Int J Refract Met Hard Mater 1998;16:217–22. https://doi.org/10.1016/S0263-4368(98)00021-3.
[29] Wei R, Langa E, Arps J, Yang Q, Zhao L. Erosion resistance of thick nitride and carbonitride coatings deposited using plasma enhanced magnetron sputtering. Plasma Process Polym 2007;4:693–9. https://doi.org/10.1002/ppap.200731707.
[30] Swaminathan VPS, Wei R, Gandy DW. Nanotechnology coatings for erosion protection of turbine components. J Eng Gas Turbines Power 2010;132. https://doi.org/10.1115/1.3028567.
[31] Avcu E, Fidan S, Yildiran Y, Sinmazçelik T. Solid particle erosion behaviour of Ti6Al4V alloy. Tribol Mater Surf Interfaces 2013;7:201–10. https://doi.org/10.1179/1751584X13Y.0000000043.
[32] Avcu E, Yildiran Y, Şahin AE, Fidan S, Sinmazçelik T. Influences of particle impingement angle and velocity on surface roughness, erosion rate, and 3D surface morphology of solid particle eroded Ti6Al4V alloy. Acta Phys Pol A 2014;125:541–3. https://doi.org/10.12693/APhysPolA.125.541.
[33] Khoddami A, Salimi-Majd D, Mohammadi B. Finite element and experimental investigation of multiple solid particle erosion on Ti-6Al-4V titanium alloy coated by multilayer wear-resistant coating. Surf Coat Technol 2019;372:173–89. https://doi.org/10.1016/J.SURFCOAT.2019.05.042.
[34] Ally S, Spelt JK, Papini M. Prediction of machined surface evolution in the abrasive jet micro-machining of metals. Wear 2012;292–293:89–99. https://doi.org/10.1016/J.WEAR.2012.05.029.
[35] Hufnagel M, Werner-Spatz C, Koch C, Staudacher S. High-speed shadowgraphy measurements of an erosive particle-laden jet under high-pressure compressor conditions. J Eng Gas Turbines Power 2018;140. https://doi.org/10.1115/1.4037689.
[36] Sahoo R, Mantry S, Sahoo TK, Mishra S, Jha BB. Effect of microstructural variation on erosion wear behavior of Ti-6Al-4V alloy. Tribol Trans 2013;56:555–60. https://doi.org/10.1080/10402004.2013.767400.
[37] Sahoo R, Mantry S, Sahoo TK, Mishra S, Jha BB. Influence of microstructure on high temperature solid particle erosion behaviour of Ti-6Al-4V alloy. Trans Indian Inst Met 2014;67:299–304. https://doi.org/10.1007/s12666-013-0347-6.
[38] Sahoo R, Jha BB, Sahoo TK, Mantry S. Effect of volume fraction of primary alpha phase on solid particle erosion behavior of Ti-6Al-4V Alloy. Tribol Trans 2015;58:1105–18. https://doi.org/10.1080/10402004.2015.1046573.
[39] Özen İ, Gedikli H. Solid particle erosion on shield surface of a helicopter rotor blade using computational fluid dynamics. J Aerosp Eng 2019;32:04018131. https://doi.org/10.1061/(ASCE)AS.1943-5525.0000962.
[40] Yan C, Chen W, Zhao Z, Liu L. A probability prediction model of erosion rate for Ti-6Al-4V on high-speed sand erosion. Powder Technol 2020;364:373–81. https://doi.org/10.1016/j.powtec.2020.01.058.
[41] Petrov YV, Bragov AM, Kazarinov NA, Evstifeev AD. Experimental and numerical analysis of the high-speed deformation and erosion damage of the titanium alloy VT-6. Phys Solid State 2017;59:93–7. https://doi.org/10.1134/S1063783417010267.
[42] Evstifeev AD, Smirnov IV. Features of solid particle erosion of metals. Phys Mesomech 2022;25:12–7. https://doi.org/10.1134/S1029959922010027/FIGURES/7.
[43] Rajamurugan G, Krishnasamy P, Bhushan GD, Jeyakumar PD. Influence of temperature, impingement angle, velocity and standoff distance on the erosion characteristics of inconel 718 and Ti-6Al-4V. Surf Rev Lett 2022;29. https://doi.org/10.1142/S0218625X22500111.
[44] Finnie I. Erosion of surfaces by solid particles. Wear 1960;3:87–103. https://doi.org/10.1016/0043-1648(60)90055-7.
[45] Sheldon GL, Finnie I. On the ductile behavior of nominally brittle materials during erosive cutting. J Manuf Sci Eng Trans Asme 1966;88:387–92. https://doi.org/10.1115/1.3672666.
[46] Goodwin JE, Sage W, Tilly GP. Study of erosion by solid particles. Proc Inst Mech Eng 1969;184:279–92. https://doi.org/10.1243/pime_proc_1969_184_024_02.
[47] Oka YI, Nishimura M, Nagahashi K, Matsumura M. Control and evaluation of particle impact conditions in a sand erosion test facility. Wear 2001;250:736–43. https://doi.org/10.1016/S0043-1648(01)00710-4.

[48] Oka YI, Ohnogi H, Hosokawa T, Matsumura M. The impact angle dependence of erosion damage caused by solid particle impact. Wear 1997;203–204:573–9. https://doi.org/10.1016/S0043-1648(96)07430-3.
[49] Neilson JHH, Gilchrist A. Erosion by a stream of solid particles. Wear 1968;11:111–22. https://doi.org/10.1016/0043-1648(68)90591-7.
[50] Bitter JGA. A study of erosion phenomena. Part II Wear 1963;6:169–90. https://doi.org/10.1016/0043-1648(63)90073-5.
[51] M.P. Polak, D. Morgan, Extracting Accurate Materials Data from Research Papers with Conversational Language Models and Prompt Engineering – Example of ChatGPT, (2023) 1–7. ⟨http://arxiv.org/abs/2303.05352⟩.
[52] M.P. Polak, S. Modi, A. Latosinska, J. Zhang, C.-W. Wang, S. Wang, , Flexible, Model-Agnostic Method for Materials Data Extraction from Text Using General Purpose Language Models, (2023). ⟨http://arxiv.org/abs/2302.04914⟩.
[53] A. Rohatgi, WebPlotDigitizer, (n.d.). ⟨https://automeris.io⟩.
[54] Committee AH. Properties and Selection: Irons, Steels, and High-Performance Alloys. ASM International; 1990. https://doi.org/10.31399/asm.hb.v01.9781627081610.
[55] D.M. Stefanescu, ed., Cast Iron Science and Technology, ASM International, 2017. https://doi.org/10.31399/asm.hb.v01a.9781627081795.
[56] Committee AH. Properties and Selection: Nonferrous Alloys and Special-Purpose Materials. ASM International; 1990. https://doi.org/10.31399/asm.hb.v02.9781627081627.
[57] 2018. K.AndersonJ.WeritzJ.G.KaufmanAluminum Science and TechnologyASM International10.31399/asm.hb.v02a.9781627082075.
[58] 2019. K.AndersonJ.WeritzJ.G.KaufmanProperties and Selection of Aluminum AlloysASM International10.31399/asm.hb.v02b.9781627082105.
[59] 2014. J.L.DossettG.E.TottenHeat Treating of Irons and SteelsASM International10.31399/asm.hb.v04d.9781627081689.
[60] 2016. G.E.TottenHeat Treating of Nonferrous AlloysASM International10.31399/asm.hb.v04e.9781627081696.
[61] 1993. D.L.OlsonT.A.SiewertS.LiuG.R.EdwardsWelding, Brazing, and SolderingASM International10.31399/asm.hb.v06.9781627081733.
[62] I. Jenkins ASM International Powder Metallurgy2015. 10.31399/asm.hb.v07.9781627081757.
[63] 2000. H.KuhnD.MedlinMechanical Testing and EvaluationASM International10.31399/asm.hb.v08.9781627081764.
[64] 2004. G.F.Vander VoortMetallography and MicrostructuresASM International10.31399/asm.hb.v09.9781627081771.
[65] Committee AH. Materials Characterization. ASM International; 2019. https://doi.org/10.31399/asm.hb.v10.9781627082136.
[66] 2018. A.AhmadL.J.BondNondestructive Evaluation of MaterialsASM International10.31399/asm.hb.v17.9781627081900.
[67] 2017. G.E.TottenFriction, Lubrication, and Wear TechnologyASM International10.31399/asm.hb.v18.9781627081924.
[68] Committee AH. Fatigue and Fracture. ASM International; 1996. https://doi.org/10.31399/asm.hb.v19.9781627081931.
[69] 2008. S.ViswanathanD.ApelianR.J.DonahueB.DasGuptaM.GywnJ.L.JorstadR.W.MonroeM.SahooT.E.PruchaD.TwarogCastingASM International10.31399/asm.hb.v15.9781627081870.
[70] 1995. M.M.GauthierEngineered Materials Handbook Desk EditionASM International10.31399/asm.hb.emde.9781627082006.
[71] 1998. J.R.DavisMetals Handbook Desk EditionASM International10.31399/asm.hb.mhde2.9781627081993.
[72] Finnie I, Wolak J, Kabil Y. Erosion of metals by solid particles. J Mater 1967;2:682–700.
[73] Ruff AW, Ives LK. Measurement of solid particle velocity in erosive wear. Wear 1975;35:195–9. https://doi.org/10.1016/0043-1648(75)90154-4.
[74] ASTM E140-12B, Standard Hardness Conversion Tables for Metals Relationship Among Brinell Hardness, Vickers Hardness, Rockwell Hardness, Superficial Hardness, Knoop Hardness, Scleroscope Hardness, and Leeb Hardness, (2019). https://doi.org/10.1520/E0140-12R19E01.1.6.
[75] Sheather SJ. Diagnostics and Transformations for Multiple Linear Regression. A Mod. Approach to Regres. with R. New York, NY: Springer; 2009. p. 151–225. https://doi.org/10.1007/978-0-387-09608-7_6.
[76] Neter J, Wasserman W, Kutner MH. Multicollinearity, iinfluential observations, and other topics in regression analysis–II. In: Richard D, Irwin INC, editors. Appl. Linear Regres. Model. Il: Homewood; 1989. p. 390–400.
[77] Söderberg S, Hogmark S, Engman U, Swahn H. Erosion classification of materials using a centrifugal erosion tester. Tribol Int 1981;14:333–43. https://doi.org/10.1016/0301-679X(81)90101-8.
[78] Finnie I. Some reflections on the past and future of erosion. Wear 1995;186–187:1–10. https://doi.org/10.1016/0043-1648(95)07188-1.
[79] Bonu V, Praveen Kumar V, Narayana C, Barshilia HC. Role of bonding nature on the temperature dependent erosion behavior of solid materials: A detailed high temperature Raman spectroscopic analysis. J Appl Phys 2020;128:015104. https://doi.org/10.1063/5.0007731.
[80] Roy M. Elevated temperature erosive wear of metallic materials. J Phys D Appl Phys 2006;39:R101–24. https://doi.org/10.1088/0022-3727/39/6/R01.
[81] Roy M, Ray KK, Sundararajan G. Erosion-oxidation interaction in Ni and Ni-20Cr alloy. Metall Mater Trans A Phys Metall Mater Sci 2001;32:1431–51. https://doi.org/10.1007/s11661-001-0232-5.
[82] Buuren S van, Groothuis-Oudshoorn K. mice: multivariate Imputation by Chained Equations in R. J Stat Softw 2011;45:1–67. https://doi.org/10.18637/JSS.V045.I03.